DELTA UNDULATOR FOR CORNELL ENERGY RECOVERY LINAC *

Alexander B. Temnykh

Cornell University, LEPP, Ithaca, New York, USA†

(Dated: November 7, 2008)

* Work supported by National Science Foundation under contract DMR 0225180

Abstract

In anticipation of a new era of synchrotron radiation sources based on Energy Recovery Linac techniques we designed, built and tested a short undulator magnet prototype whose features make optimum use of the unique conditions expected in these facilities. The prototype has pure permanent magnet (PPM) structure with 24mm period, 5mm diameter round gap and is 30cm long. In comparison with conventional undulator magnets it has

- *Full X-ray polarization control.* It may generate varying linear polarized as well as left and right circular polarized x-rays with photon flux much higher than existing Apple-II type devices.
- 40% *stronger magnetic field* in linear and approximately *2 times stronger* in circular polarization modes. This advantage translates into higher x-ray flux.
- *Compactness.* The prototype can be enclosed in a $\sim$ 20cm diameter cylindrical vacuum vessel.

These advantages were achieved through a number of non-conventional approaches. Among them is control of the magnetic field strength via longitudinal motion of the magnet arrays. The moving mechanism is also used for x-ray polarization control. The compactness is achieved using a recently developed permanent magnet soldering technique for fastening PM blocks. We call this device a "Delta" undulator after the shape of it's PM blocks.

The presented article describes the design study, various aspects of the construction and presents some test results.

PACS numbers: 85.70.-w, 41.60.-m, 07.85.Qe

[†]Mail send to: A. Temnykh, Wilson Lab, Cornell University, NY 14850, USA

E-mail abt6@cornell.edu , tel. +1 607 255 4882, fax +1 607 255 8062

I. INTRODUCTION

Synchrotron radiation facilities based on Energy Recovery Linacs will have a number of specific features, which could be exploit for superior insertion device design. In comparison with storage rings, they will have smaller horizontal beam emittance and consequently smaller horizontal beam size. In addition, they will not require extra beam aperture to provide space for residual oscillation of the injected particles. Furthermore, ERL facilities can tolerate a much bigger one-pass beam loss than storage rings that require adequate beam life time. All this makes possible a reduction of horizontal beam aperture to the size of the vertical, i.e., the beam aperture can be round. Round gap (bore) insertion devices, in turn, may significantly facilitate the design as well as enhance magnetic field properties. Following this argument we chose a 5mm diameter round bore. The roundness provides symmetry of the design and a 5mm diameter seemed to be large enough for access for magnetic field measurements.

Field strength is controled by an adjustable phase (AP) scheme. In this scheme the peak field is controlled by moving the magnetic arrays relative to each other in the longitudinal direction. The AP scheme is compact and does not require a large external frame to hold magnet arrays and for gap control. Moreover, the mechanism providing magnetic array longitudinal motion, can be used for x-ray polarization and photon spectrum control. The AP scheme's theoretical model has been developed by Roger Carr in references [2] and [3]. Electron beam test results were described in [4]. Presently, one AP type undulator successfully operates as a x-ray source for the "ADRESS" beam line at Swiss Light Source. This undulator provides x-rays in the energy range between 400 eV and 1800 eV with circular and variable linear polarization see website [5].

The round bore allows the design of a highly symmetric magnetic structure. On the one side, magnetic structure can be considered as combination of two identical undulators rotated by 90^0 relative to each other around beam axis. On the other, it can also be considered as a kind of Apple-III structure mentioned in reference [8]. The "Delta" structure has similarities with the undulators described in [6] and [7] as well. The structure can provide $\sqrt{2}$ times stronger planar magnetic field than conventional planar PPM undulators and approximately two times stronger helical field if compared with existing Apple-II type undulators of the same gap to period ratio.

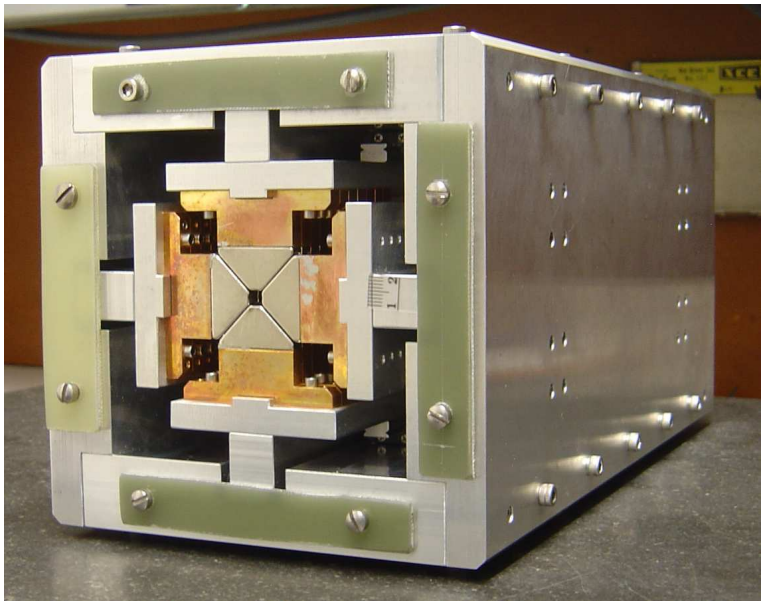

FIG. 1: "Delta" undulator prototype view

The newly developed PM magnet block fastening technique is the key to the design compactness. Mechanical fastening methods were considered as not very practical, because they would take additional space and, probably, would require more complex magnetic block shape. The latter could considerably increase the cost and the realization time of the project. Gluing was also undesirable because it would not be comptible with in-vacuum operation. After appropriate investigation we developed a technique for soldiering of Ni coated NdFeB (40SH) magnets to copper holders without demagnetization [9]. This technique was used in the construction.

It should be mentioned that the conceptual idea for a such PPM undulator was presented in 2006 [1]. Encouraged by interest from Cornell x-ray users community, this idea evolved into a detailed design and recently a prototype was built and tested.

II. MODEL DESCRIPTION

A. General information

A picture of the "Delta" undulator prototype is shown on Fig.1. The prototype is ∼30cm long, ∼ 15cm high and ∼ 15cm wide. The magnetic structure consists of two pairs of magnetic arrays as depicted computer generated Fig.2 with major components numbered.

One pair provides vertical field and another horizontal. Magnet arrays (1) are assembled on

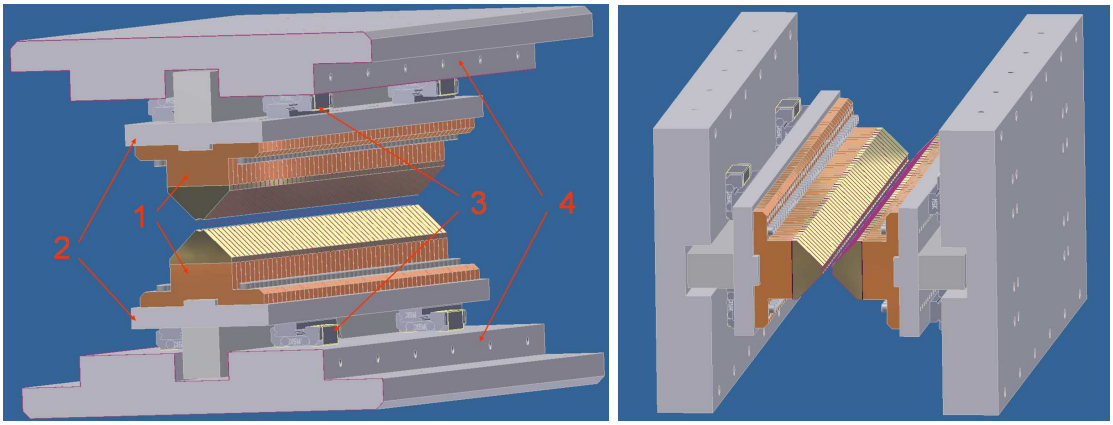

FIG. 2: Computer generated view. Left plot - magnetic arrays providing vertical field. Here (1) - magnetic arrays, (2) - base plates, (3) - rails providing longitudinal motion, (4)- plates forming the rigid frame. Right plot - arrays providing horizontal field.

base plates (2). To provide longitudinal displacement for the field strength and polarization control, these plates are mounted on miniature rails (3) attached to the thick plates forming a rigid frame. In linear polarization mode the pairs will be in phase, so the resulted field will be planar and will be $\sqrt{2}$ stronger than from a single pair. In circular polarization mode the pairs will be shifted relative to each other by 1/4 period or 90^0, so the resultant field will be helical. To change the field strength, two arrays forming the pair should be shifted longitudinal in opposite directions. The prototype has a 5mm diameter bore. Gas conductance from the central region is provided by four 0.5mm wide slits between magnetic arrays. From the following discussion it will be seen that these slits have enough conductance to provide satisfactory vacuum conditions on beam axis. Note that the picture on Fig. 1 shows the prototype without magnetic array driving mechanisms. These mechanisms are designed and are in process of construction. They will be added latter.

B. Magnetic field properties

A 3D model of one period of the "Delta" type magnetic structure used in magnetic field calculation by code "Vector Fields" is shown in Fig. 3. As a real structure the model had 24mm period, 5mm diameter bore and 0.5mm wide slits between magnetic arrays, permanent magnet material characteristics of NdFeB (40SH) material ($B_r = 1.26T$) used in

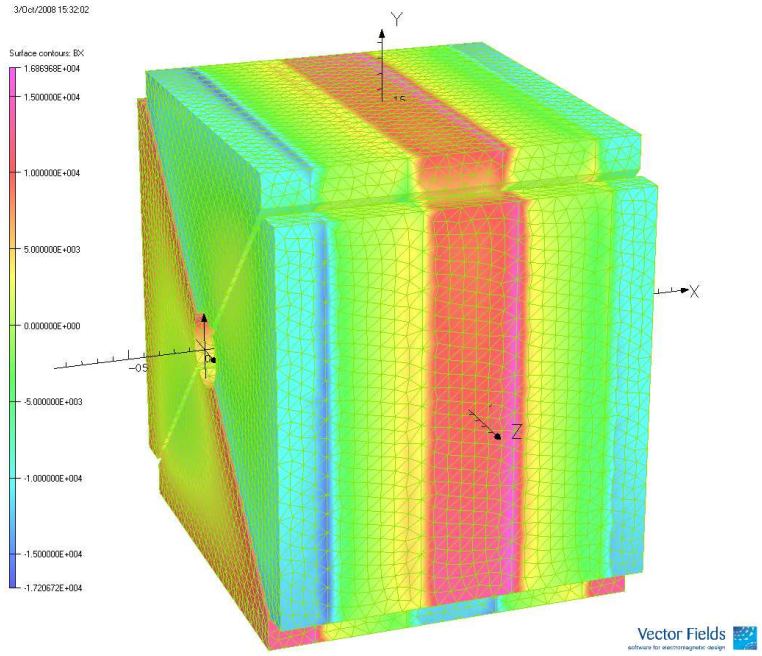

FIG. 3: 3D model of one period of "Delta" undulator magnetic structure used in field calculation

prototype construction. We calculated a field distribution along the beam axis as well as a field variation across the bore for both helical and planar modes. Field distributions have been used for calculation of x-ray spectrum and the field variation will be used for evaluation of requirement on undulator alignment and for beam dynamics study.

Plots on Fig. 4 characterize the helical mode. They depict magnetic field components on

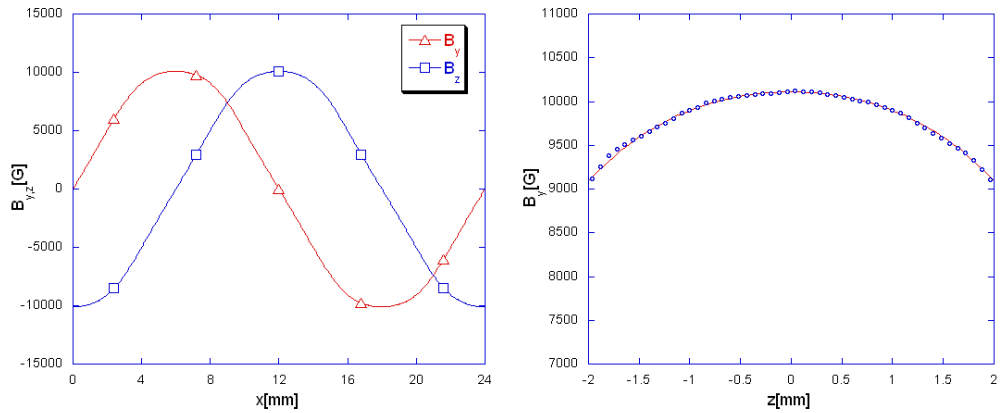

FIG. 4: Helical mode. Left plot - vertical and horizontal field components along beam axis, $Bmax = 1.01$T. Right plot - field variation across the bore. In $\pm$1mm region field variation $dB/B \simeq -0.020 \times d^2$, where d is a distance from beam axes in mm

beam axis versus longitudinal coordinate (left) and field variation across the bore (right). The left plot indicates $\simeq$ 1T peak field and 90^0 phase shift between vertical and horizontal components. The field variation dB/B across the bore, see right plot, in $\pm$1mm region around axis can be approximated as $dB/B \simeq -0.02 \times d^2$, where d is a distance from axes in mm.

Figure 5 depicts magnetic field characteristics in the planar mode. In this mode the

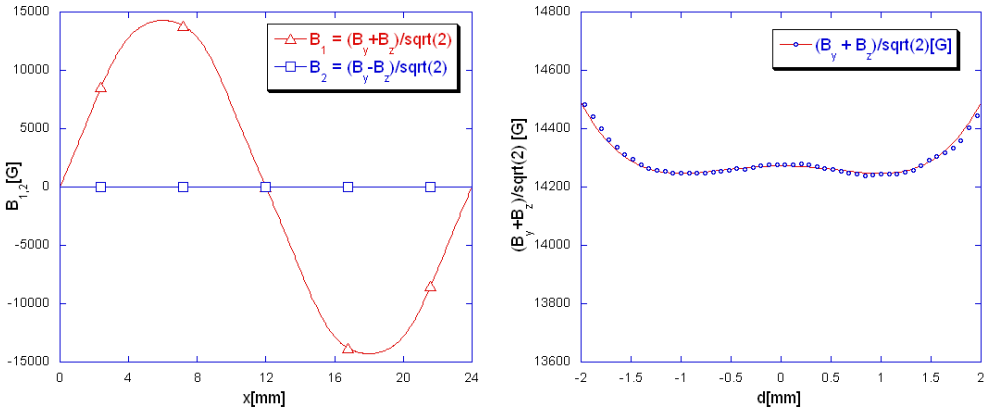

FIG. 5: Planar mode. Left plot - two orthogonal field components versus coordinate along beam axis, $Bmax \simeq 1.43$T. Right plot - field variation across the bore. In $\pm$1mm region the field variation $dB/B \simeq -0.0037 \times d^2$, where d is the distance from beam axis in mm.

vertical and horizontal field components are in phase. The left plot shows two orthogonal field components $(B_y + B_z)/\sqrt{2}$ and $(B_y - B_z)/\sqrt{2}$ on beam axis as a function of longitudinal coordinate. The first component has maximum $\sim$ 1.43T, the second is "zero". The field variation in the $\pm$1 mm region around beam axis can be described as $dB/B \simeq -0.0037 \times d^2$, where d is a distance from axes in mm.

To provide data for the possible optimization we calculated dependence of the peak field on period for both helical and planar modes. The data plotted on Fig. 6(left) was fitted with commonly used approximation

$$B[T] = a \exp\left[b\frac{g}{\lambda_0} + c\left(\frac{g}{\lambda_0}\right)^2 \right] \qquad (1)$$

where λ_0 - period and g - gap, (see references [10] and [8]). The fit yielded coefficients depicted in the Table I.

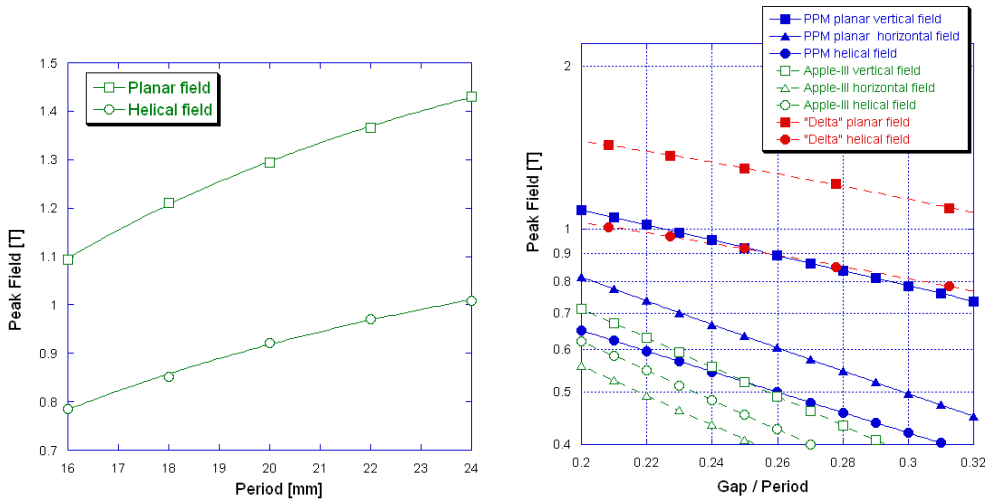

FIG. 6: Left plot - peak field in planar and helical mode as a function of period for 5mm diameter bore and magnetic material with $B_r = 1.26$T consisting with NdFeB (40SH) specification. Right plot - peak field versus gap over period ratio for "Delta" and others magnetic structures.

Mode	a	b	c
Planar field	1.96	-0.82	-3.31
Helical field	1.45	-1.28	-2.24

TABLE I: Peak field fit parameters for "Delta" undulator.

Plots on Fig. 6(right) compare the calculated peak field for "Delta" type of structure as a function of gap over period ratio with others. Data for "PPM planar vertical/horizontal field" and "PPM helical field" were found in reference [10], characteristics for Apple-III structure are from [8]. This comparison evidently show advantage of the "Delta" type structure.

C. Mechanical considerations

Dimensions of main elements such as base plates and plates forming the rigid frame where chosen after extensive stress analysis with the programs "Inventor" [11] and "ANSYS" [13]. Magnetic field calculations indicated that magnetic forces will be applied to PM blocks mostly in the region adjacent to the beam axis. In helical mode, the forces will be directed toward the beam axis and will be approximately 45N per structure period. This will cause the

base plate deformation shown in Fig.7(left) with 2μm maximum. In planar mode magnetic

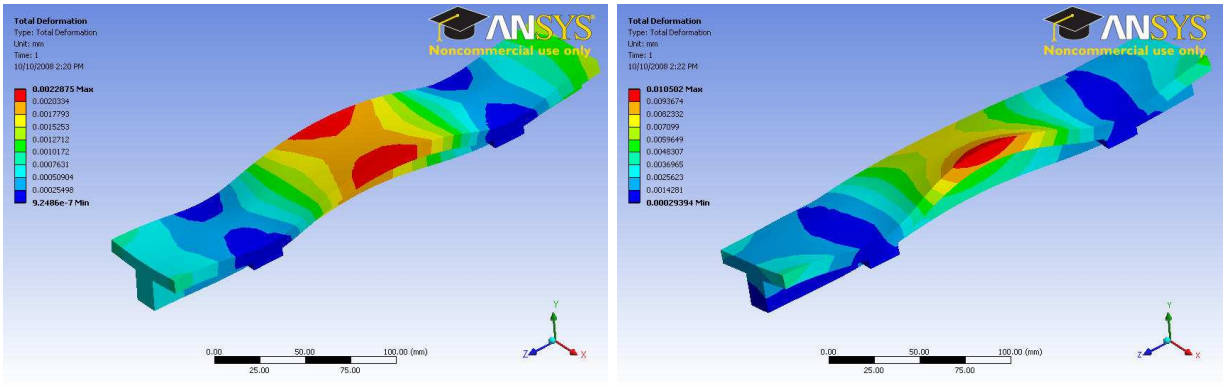

FIG. 7: Base plate deformation in helical (left plot) and planar field (right plot) modes

forces will be quit different. In addition to the $45N$ directed to the beam axis there will be an additional $282N$ perpendicular to the axis due to repulsing and attracting from the adjoint arrays. The later will produce 659N-cm torque. The resultant deformation will have a profile shown on Fig. 7(right) with 10μm maximum. This is larger than in the case of the helical mode, but still acceptable. Note that base plate deformations were minimized by optimizing the mounting rail locations.

This analysis also indicated that in the helical mode mounting rails will be stressed by 116N and in the planar by 800N forces. In the prototype we used mounting rails LU09AR from "NSK NIPPON SEIKO" rated up to 1700N of static load.

The rigid frame deformation calculated for the helical and planar modes is given Fig. 8. In the case of the helical field the maximum frame deformation will be less than 1μm and can be neglected. In the planar mode the frame deformation will be much larger, $\sim 20\mu$m. However, because it is uniform along the beam axis it will not cause variation of the field and undulator "K" parameter which could degrade the x-ray spectrum.

D. Beam heat load analysis

In "Ultrafast" mode (extreme case) the Cornell ERL will operate with 1nC per bunch charge, 1MHz repeatition rate and 0.1psec bunch duration. Following reference [12] we estimated that in this mode the heat load generated by the beam image current in the walls of 5mm diameter bore will be 28W/m. For wall conductance we assume $6 \times 10^7 [1/\Omega/m]$ for

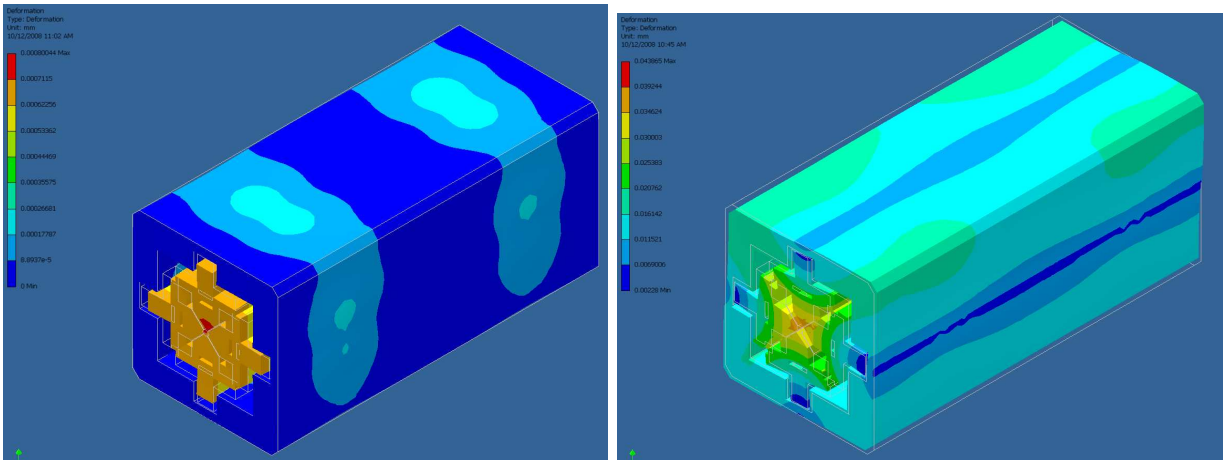

FIG. 8: Frame deformation for helical (left plot) and planar (right plot) modes of operation.

Ni coated thin copper tape placed on the top of PM blocks.

To provide a heat sink two cooling elements will be attached to both sides of the base plate as shown on Fig. 9. Using software "ANSYS" we found that under these conditions

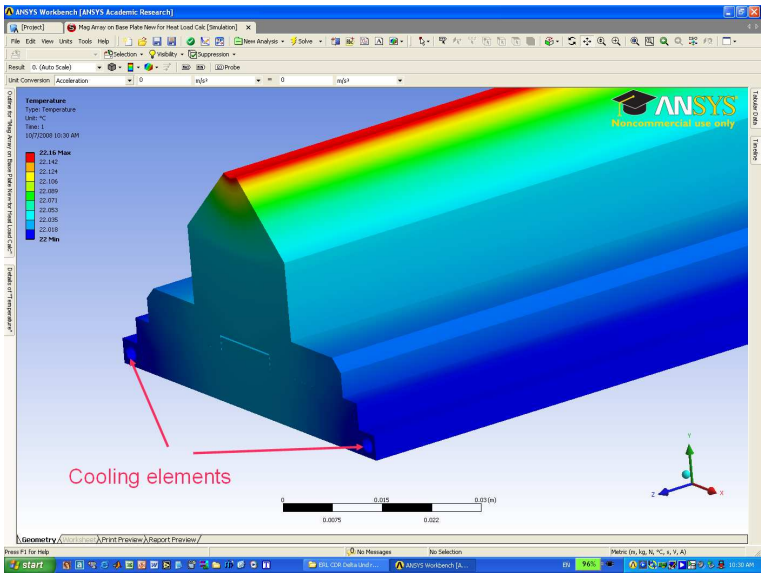

FIG. 9: Heat load analysis

the maximum temperature rise will occur at the top of the magnet array and will not exceed 0.2^0C, see Fig. 9, which is acceptable.

E. Vacuum on beam axis

As an in-vacuum device, the vacuum performance of the "Delta" undulator magnet must be evaluated to ensure compatibility with the ultra-high vacuum (UHV) requirement of the accelerator. To reduce damage from the synchrotron radiation, proper synchrotron radiation (SR) masking at the undulator entrance will prevent the direct SR strike of the undulator bore. Thus there is no beam induced dynamic gas load in the magnet bore. One only need to concern about the static residual pressure due to the thermal outgassing from the magnet pole materials. Tests [15] showed that with proper cleaning and degassing (through preassembling bakeout), Ni plated PM blocks the thermal outgassing rate can be reduced to below $4 \times 10^{-12} Torr - liter/sec/cm^2$, comparable with commonly used UHV materials such as stainless steel and copper. To prevent pressure build-up along the very small magnet bore, four 0.5-mm wide venting gaps are designed into the magnet structure to connect the bore to the outer vacuum space, where adequate vacuum pumping is installed. Simple gas transport calculation (using gas conductance formula given in [14]) shows that these venting gaps are sufficient to keep pressure in the magnet bore below $10^{-9} Torr$. For the actual insertion device (with much longer magnet length), more careful pressure calculations are planned, using 3D Monte-Carlo code (such as MOLFLOW [19]).

III. SOME ASPECTS OF THE PROTOTYPE CONSTRUCTION AND TEST RESULTS

PM blocks used for the "Delta" undulator prototype were ordered from "Stanford Material Corp". They are "Delta" like in shape and made of NbFeB 40SH material coated with $\sim 12\mu$m of Ni-Cu-Ni. All block dimensions and detailed material specification are given on Fig. 10. The blocks were fastened to copper holders by a recently developed soldering method described in [9]. As solder we used 63/37 Sn/Pb alloy with rosin component and with melting point $183^0 C$. The given alloy has a tensile strength 54MPa which is much higher than for solders with lower melting temperature. To prevent PM demagnetization during the temperature rise needed for solder melting, the blocks were surrounded by steel plates. The steel redistributed magnetic field in such way that demagnetizing field was reduced. This allowed raising the temperature above the solder melting point without risk of

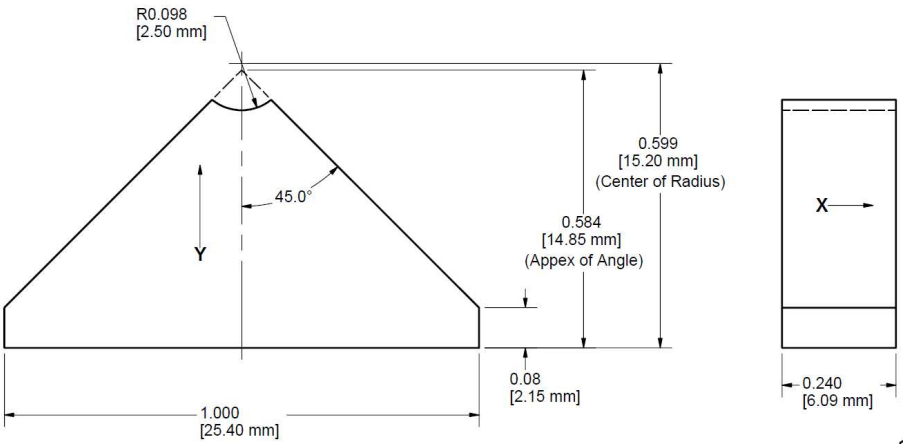

Demagnetization curves at different temperatures N40SH

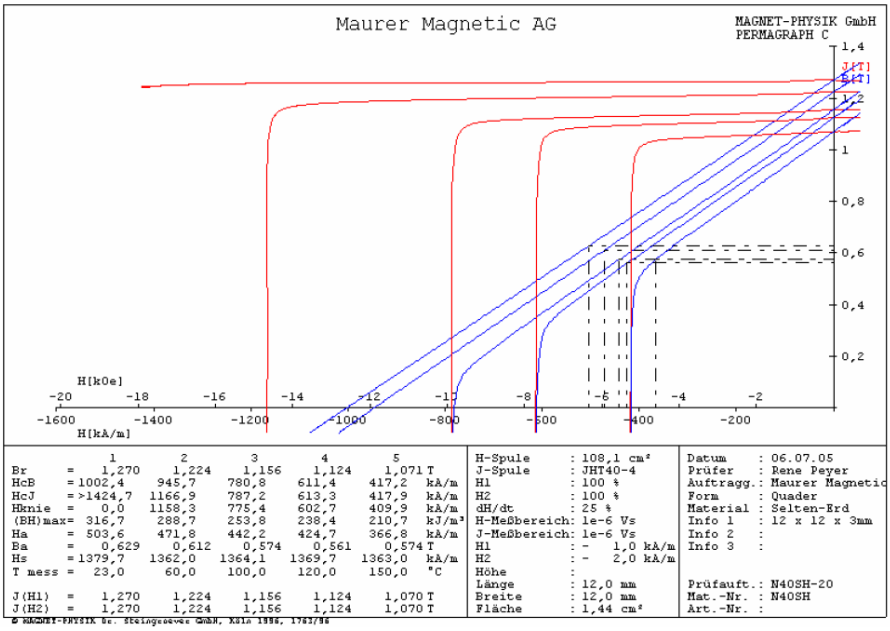

FIG. 10: PM dimensions and material specification. Material specification data was copied from "Maurer Magnetic AG" web site.

PM demagnetization. More details can be found in [9].

In the construction process PM blocks together with copper holders were enclosed in "steel jackets". The solder wire was flattened and inserted between them. Then the whole assembly was placed in oven for 2 hours at 195^0C. With 3 sets of the soldering fixture one person soldered 3 blocks in 3 hours.

A single "Delta" shape PM block and the block soldered to the copper holder are shown on Fig. 11. Note the holder has provision for mechanical fastening to the base plate and for vertical position control.

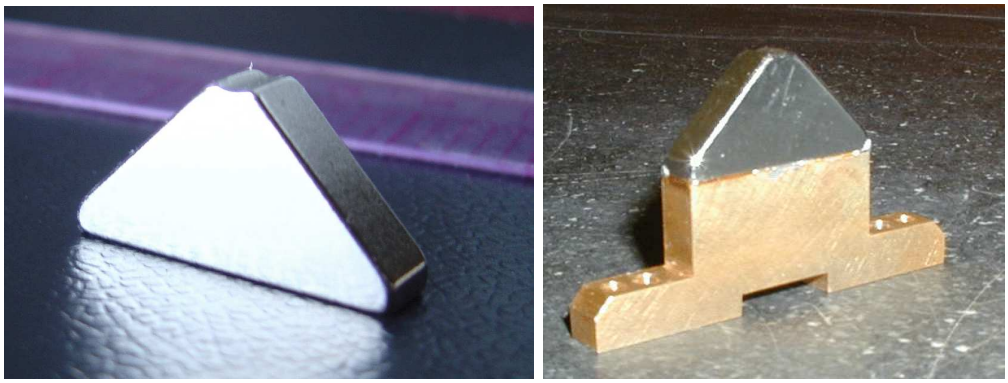

FIG. 11: Single "Delta" shape magnetic block (left), the block soldered to copper holder(right).

A. Magnetic field tuning results

The magnetic field of each of the four magnet arras has been measured with a Hall probe and tuned. The measurement setup consisted of a linear sliding stage, temperature compensated Hall probe, "LakeShore 455 DSP Gaussmeter" in connection with "HP3456A Digital Voltmeter" and stepping motor controller. For measurement control we used laptop "IBM ThinkPad" with LabView. The field was measured "on the fly" with 0.25mm step. For field analysis we used "B2E V3.3" software developed by ESRF ID group. Because of small size and weight the magnetic array was mounted on the moving stage while the Hall probe position was fixed. This configuration provided more stable measurement. Prior to the field measurement the setup was very carefully aligned.

Fig. 12 gives the setup view. Here one can see the magnet array consisted of "Delta" shaped PM blocks. The array situated on the moving linear stage while the Hall probe is fixed. At the end of array there are two vertically displaced PM blocks. This displacement has been made for "end termination" purpose.

In the process of the field tuning we first measured the field, then analyzed it with "B2E" software. In the analysis we used the doubled field strength assuming an identical array placed symmetrically relative to the Hall probe above the tested. Trajectory corrections were made by displacing the vertically magnetized blocks, phase was corrected by the blocks magnetized along beam axis. These steps, measurement and correction, were repeated until trajectory and phases converged to a satisfactory level. Usually this occurred after 10 - 15 iterations.

Fig. 13 illustrates magnet array "1" tuning result. The first plot shows the measured

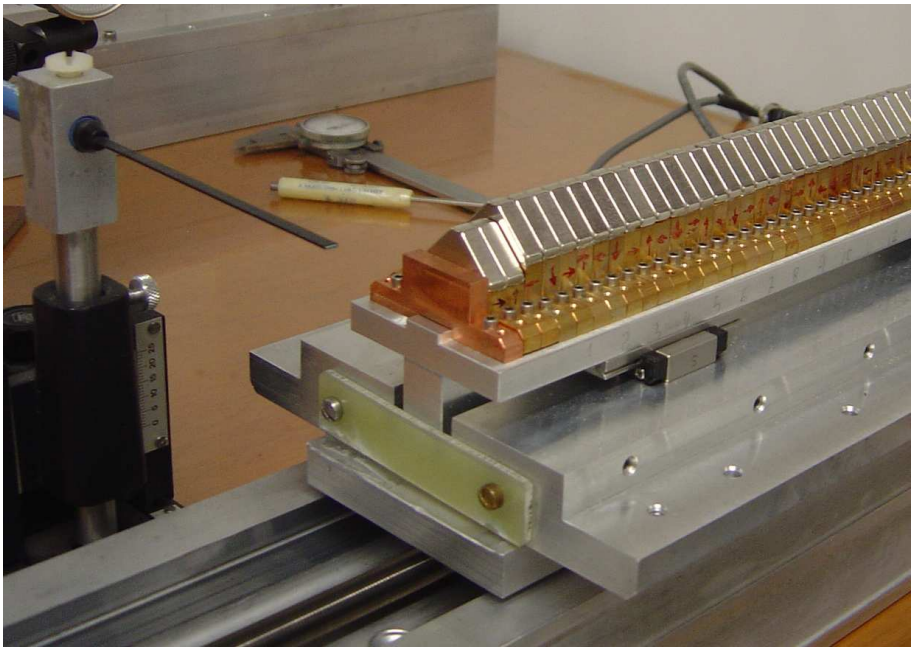

FIG. 12: Assembled array on the field measurement bench.

field. Two others are trajectory and phase errors calculated for the doubled strength field. Both indicate satisfactory results. After the field tuning, three other arrays "2", "3" and "4" had similar trajectory and phase errors.

B. Composite field analysis

Because of linearity of the PPM structure we can obtain the properties of the assembled undulator by combining individual array fields. Plots on Fig. 14 show this field for helical (left plot) and linear (right plot) modes of operation. One can notice that the peak field for both modes are in good agreement with predicted 1T and 1.4T field respectively, see subsection "Magnetic field properties". In linear mode RMS phase errors of the composed field was found to be $\sim 2.2^0$. This proves our method for individual arrays field tuning procedure.

The high field quality was also confirmed by calculation of the photon flux spectrum with program "SPECTRA" [16]. Using field distributions combined from the measurements described above and corresponding to helical and planar modes, see Fig. 14, we calculated the spectrum of the photon flux coming through a 1mm diameter slit at 50m from the source generated by electron beam with 25mA current, 8×10^{-12} m*rad emittance and $0.0002\sigma_e/E_0$

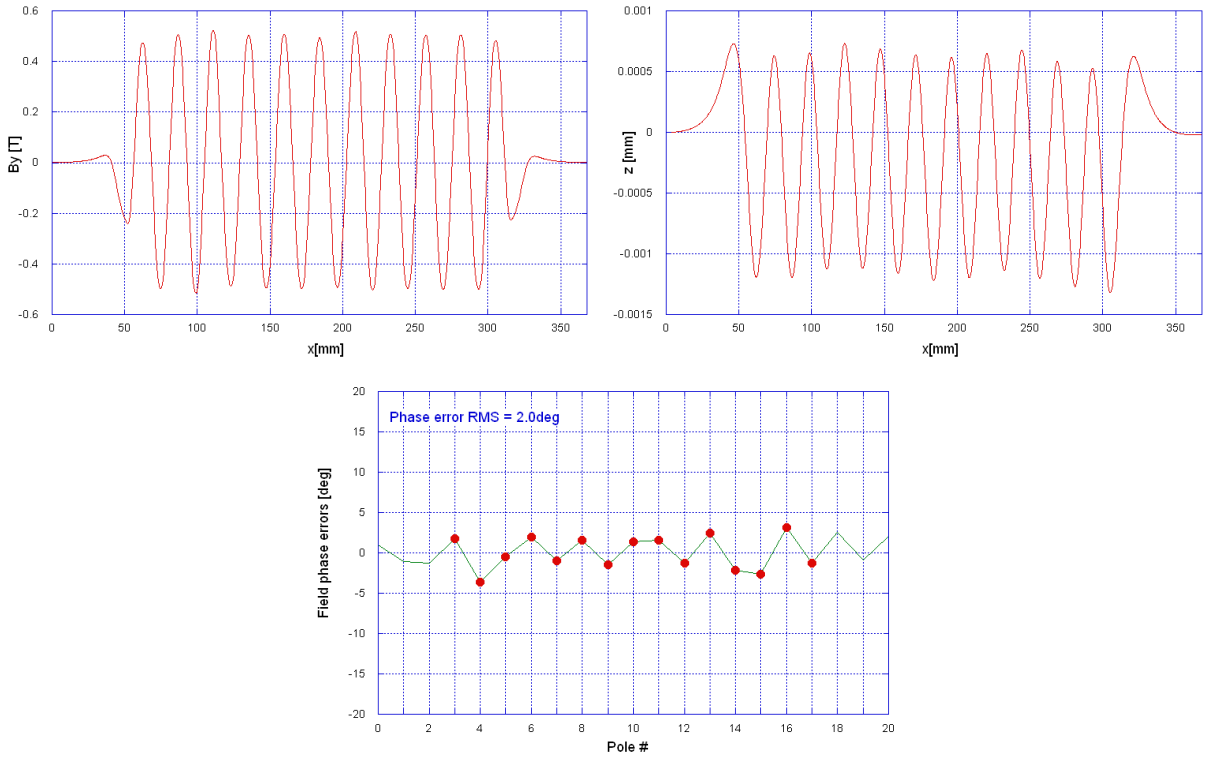

FIG. 13: Top plot - Array "1" measured magnetic field; middle and bottom plots are beam trajectory and phase errors calculated for doubled field. RMS phase errors $\sim 2.0^0$

energy spread. Those beam parameters are consisted with Cornell ERL "Coherence" mode operation. Results are plotted on Fig. 15. The left plot shows the spectrum of circular polarized photon flux corresponding to a helical field. There is only one peak at ~ 1650eV photon energy. The absence of the other peaks confirms the magnetic field quality. The right plot gives the spectrum for linear x-ray polarization corresponding to a planar field distribution. The lowest peak at ~ 1650 eV matches first undulator harmonic. Other peaks correspond to higher order odd and even harmonics. Even harmonics appeared because of the finite slit size. The well defined narrow peaks up to 15th order indicate small phase errors in the field distribution and confirm the field quality.

IV. NEXT STEPS

Prior to the full scale "Delta" undulator design and construction the following steps will be taken.

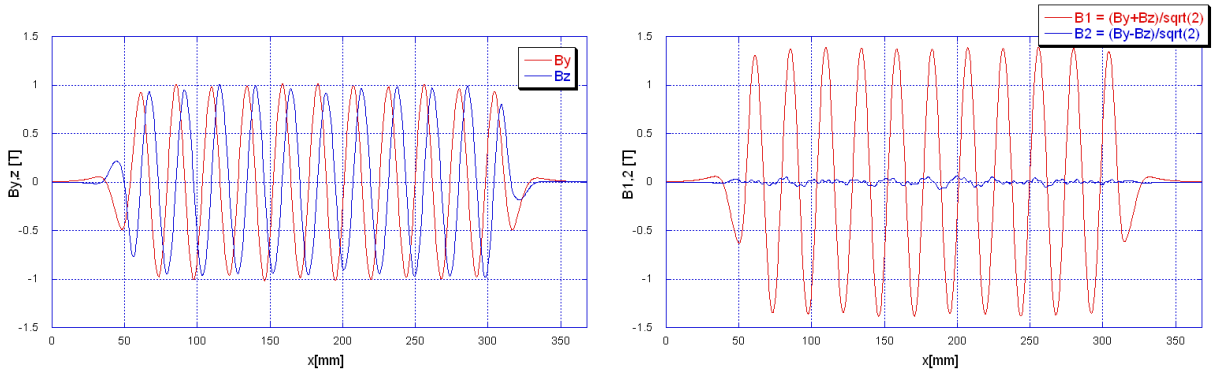

FIG. 14: Prototype field obtained as a combination of the individual array fields. Left plot shows vertical and horizontal field components for magnet arrays in helical mode configuration. Right plot gives two orthogonal field components for magenetic arrays in planar mode position. For latter RMS phase errors $\sim 2.2^0$

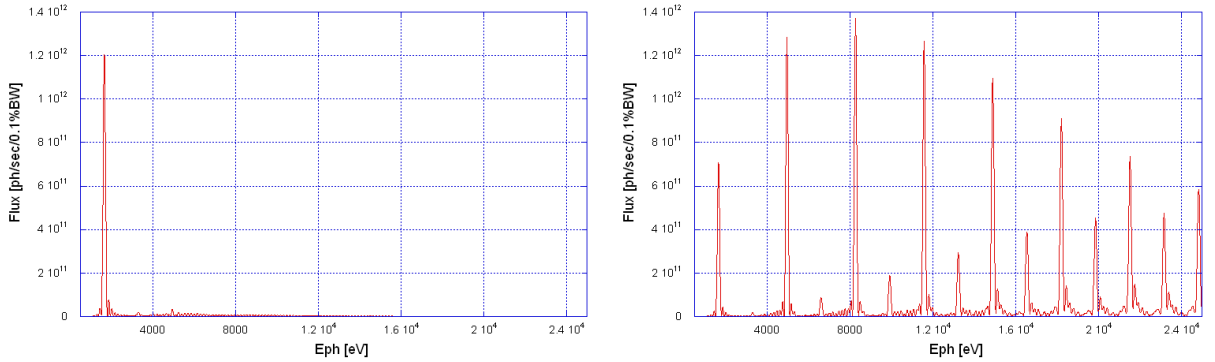

FIG. 15: Spectrum of the photon flux calculated for the composite field distributions corresponding to the helical (upper) and planar (bottom) mode of operation.

In order to verify magnetic field properties inside the 5mm diameter undulator gap we will built a special magnetic field measurement setup. In this setup a small size Hall probe will be inserted in the bore and moved along the beam axis. This project is now under way.

To provide the smooth flow of the beam image current between 24mm (1in) diameter ERL beam pipe and 5mm diameter undulator bore we have to design special transition pieces. They will be carefully examined for the beam impedance and beam induced power dissipation.

Because we are going to use the "Delta" undulators for in-vacuum operation, we will develop and test vacuum cleaning techniques suitable for all undulator components. Tradi-

tional in-vacuum high temperature baking at 140^0C can be applied to all components except of magnet arrays. Magnetic arrays can be stabilized against demagnetization at 120^0C by attaching ferromagnetic plates as described in reference [17]. We also will exam the vacuum properties of the joints between PM blocks and holders where we used Sn/Pb alloy for soldering.

In the "Delta" undulator prototype, magnet arrays will be moved manually using a large screws. For the real undulator we will design mechanisms based on ball screws driving with stepping motors.

In the course of the full scale undulator design study the transvers and longitudinal beam impedance will be investigated with 3D simulation codes "MAFIA" [18]. There will also be considered effect of the bore roughness. The residual gas pressure distribution will be simulated with code "Molflow" [19].

Coherent synchrotron radiation (CSR) for wave length larger than bunch length is shielded by narrow beam pipe (undulator bore), but because of the slits between magnet arrays the effective beam pipe of "Delta" undulator might be quit large. We will therefore investigate intensity of CSR radiation and possibilities to suppress it.

V. CONCLUSION

We have developed, built and tested a "Delta" type undulator prototype which exploits properties of an ERL type beam. In the design we used non-traditional approaches which led to a number of advantages of the prototype over conventional undulator magnets. Among them are stronger magnetic field, very flexible x-ray polarization control and compactness. The stronger magnetic field translates to the higher photon flux.

Experience obtained in the course of the work on the prototype will help us build the full scale device.

It should be noted that the "Delta" type undulator can also benefit free electron laser facilities with beam parameters similar to those of ERLs.

VI. ACKNOWLEDGEMENTS

I would like to thank David Rice, Sol Gruner, Donald Bilderback and Maury Tigner for support of the described activity. My special thanks to Georg Hoffstaetter, Yulin Li and Kenneth Finkelstein for useful discussions and help.

This work has been supported by NSF grant DMR 0225180.

[1] A. Temnykh, Helical PPM Undulator for ERL, CBN 06-2, Cornell 2006. URL : $http$: $//www.lns.cornell.edu/public/CBN/2006$

[2] Roger Carr, Adjustable phase insertion devices as X-ray sources, Nucl. Instr. And Meth. A 306(1991) 391-396

[3] Roger Carr and Heinz-Dieter Nuhn, Design study for an adjustable phase undulator, Rev. Sci. Instrum. 63 (1), January 1992, pp. 347-351

[4] Roger Carr, et al., First Test Results for an Adjustable Phase Undulator. In Proceedings of 1992 EPAC, p.489

[5] URL : $sls.web.psi.ch/view.php/beamlines/adress/source$

[6] Hideo ONUKI, ELLIPTICALLY POLARIZED SYNCHROTRON RADIATION SOURCE WITH CROSSED AND RETTARDED MAGNETIC FIELDS, Nucl. Instr. And Meth. A 246(1986) 94-98

[7] Pavel Vobly, HELICAL UNDULATOR FOR PRODUCING CIRCULARLY POLARIZED PHOTONS, In proccedings of the workshop on new kinds of positron sources for linear collider, March 4-7, 1997. SLAC-R-502, CONF-970374, pp. 429-430

[8] J. Bahrdt, et al., UNDULATORS FOR THE BESSY SOFT-X-RAY FEL, Proccedings of the 2004 FEL Conference, pp. 610-613.

[9] A. Temnykh, Permanent Magnet Temporary Demagnetization Temperature Rise Technique and their Application for Soldering, CBN 07-13, Cornell 2007. (Patent pending)

[10] P. Elleaume, et al., Design considerations for a 1 A SASE undulator, Nucl. Instr. And Meth. A 455(2000) 503-523

[11] 2008 Autodesk, Inc.

[12] O. Henry, O. Napoly, The Resistive-Pipe Wake Potentials for Short Bunches Part. Acc., 1991, Vol. 35, pp 235-247

[13] ANSYS, Inc

[14] John F. O'Hanlon, A Users Guide to Vacuum Technology, Second Edition, pp.33 - 37

[15] Yulin Li, ADC In-Vacuum Undulator Magnet Material Outgassing Test Report Feb. 20, 2008

[16] T. Tanaka and H. Kitamura, J. Synchrotron Radiation 8(2001)1221

[17] A. Temnykh, Vacuum Baking Test of NdFeB Permanent Magnet Material for ERL Undulators,

CBN 07-4, Cornell 2007.

[18] MAFIA, the general purpose electromagnetic code produced by THD-DESY-KFA collaboration, T. Weiland, 6100 Darmstadt, Germany.

[19] R. Kersevan, et al., CALCULATION, MEASUREMENT AND ANALYSIS OF VACUUM PRESSURE DATA AND RELATED BREMSSTRAHLUNG LEVELS ON STRAIGHT SECTIONS OF THE ESRF, Proceedings of EPAC 2006, Edinburgh, Scotland